Chemistry & Biology, Vol. 11, 1701–1707, December, 2004, ©2004 Elsevier Ltd. All rights reserved. DOI 10.1016/j.chembiol.2004.10.011

The Use of Carbohydrate Microarrays to Study Carbohydrate-Cell Interactions and to Detect Pathogens

Matthew D. Disney and Peter H. Seeberger*
Laboratory for Organic Chemistry
Swiss Federal Institute of Technology Zürich
ETH Hönggerberg HCI F315
Wolfgang-Pauli-Strasse 10
8093 Zürich, Switzerland

Summary

The use of carbohydrate microarrays to investigate the carbohydrate binding specificities of bacteria, to detect pathogens, and to screen antiadhesion therapeutics is reported. This system is ideal for whole-cell applications because microarrays present carbohydrate ligands in a manner that mimics interactions at cell-cell interfaces. Other advantages include assay miniaturization, since minimal amounts (~picomoles) of a ligand are required to observe binding, and high throughput, since thousands of compounds can be placed on an array and analyzed in parallel. Pathogen detection experiments can be completed in complex mixtures of cells or protein using the known carbohydrate binding epitopes of the pathogens in question. The nondestructive nature of the arrays allows the pathogen to be harvested and tested for antibacterial susceptibility. These investigations allow microarray-based screening of biological samples for contaminants and combinatorial libraries for antiadhesion therapeutics.

Introduction

Carbohydrates displayed on the surface of cells play critical roles in cell-cell recognition, adhesion, signaling between cells, and as markers for disease progression. Neural cells use carbohydrates to facilitate development and regeneration [1]; cancer cell progression is often characterized by increased carbohydrate-dependent cell adhesion and the enhanced display of carbohydrates on the cell surface [2]; viruses recognize carbohydrates to gain entry into host cells [3]; and bacteria bind to carbohydrates for host cell adhesion [4]. Identification of the specific saccharides involved in these processes is important to better understand cell-cell recognition at the molecular level and to aid the design of therapeutics and diagnostic tools.

Many interactions at cell-cell interfaces involve multiple binding events that occur simultaneously [5, 6]. This "multivalent" type of binding amplifies affinities relative to interactions that involve only a single ligand [6]. This effect has led to the development of multivalent antiadhesive therapeutics against bacteria [7, 8] and viruses by displaying carbohydrates on flexible polymers [9–11]. Dendrimers and bovine serum albumin (BSA) have also been used as multivalent scaffolds [8]. Additionally, devices that are responsive to the presence of a pathogen use multivalent binding for recognition [12, 13, 14].

The use of carbohydrate microarrays to study the interactions of bacteria with carbohydrates is reported. Cell-surface carbohydrates are exploited by many pathogens for adherence to tissues and entry into host cells. Microarrays present carbohydrates in an ideal manner to study cell-cell interactions because they can accommodate multivalent binding. Our results show that, after incubation of *Escherichia coli* with a carbohydrate array presenting a variety of monosaccharides, binding of the bacterium is observed to mannose on the array. Binding can also be observed when the bacterium is present within heterogeneous solutions of cells or protein. These results suggest that arrays can be used to detect pathogens. Bacteria captured by the arrays can also be harvested and tested for antibiotic susceptibility. In addition, we also show that rapid screening of potential antiadhesion therapeutics can be facilitated with this platform. The miniaturized and high-throughput nature of microarrays makes them a promising tool to screen combinatorial libraries for discovery of antiadhesion therapeutics, test organisms for their carbohydrate binding epitopes, and to detect pathogens. Since carbohydrate-cell interactions are ubiquitous in nature, these investigations have the potential to impact a variety of important areas.

Results and Discussion

Cell Adhesion to Carbohydrate Arrays

Five different monosaccharides equipped with an ethanolamine linker on their reducing ends were used to construct the carbohydrate arrays (Figure 1). Functionalized sugars were spotted onto glass slides that had been coated with the amine-reactive homobifunctional disuccinimidyl carbonate linker. In initial tests, 10 μl of a 20 mM carbohydrate solution was placed onto different positions on the surface. Slides were hybridized with 10^9 *E. coli* (ORN178) cells that had been stained with a nucleic acid staining dye (Figure 2). After removing unbound bacteria by washing, slides were scanned using a fluorescent array scanner. Results show that a strongly fluorescent signal (signal to noise [S/N] >10) was observed at positions where mannose was immobilized; hybridization with unstained *E. coli* resulted in a weak signal (S/N ~2). The remainder of the slide exhibited no signal above background (data not shown).

Next, an arraying robot was used to construct high-density arrays. The robot spatially delivered 1 nl of carbohydrate-containing solutions that ranged in concentration from 20 mM to 15 μM, and the resulting spots had a diameter of ~200 μm. Several types of slides were tested to optimize array performance. Standard amine-coated glass slides were reacted with either disuccinimidyl carbonate or disuccinimidyl tetrapolyethylenglycol linkers, alternatively CodeLink polymer coated slides were used (data not shown). For each of these

*Correspondence: seeberger@org.chem.ethz.ch

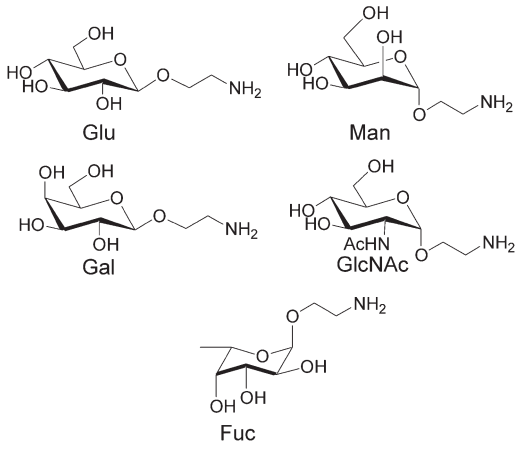

Figure 1. Carbohydrates Used to Construct the Microarrays and to Study Interactions with Bacteria

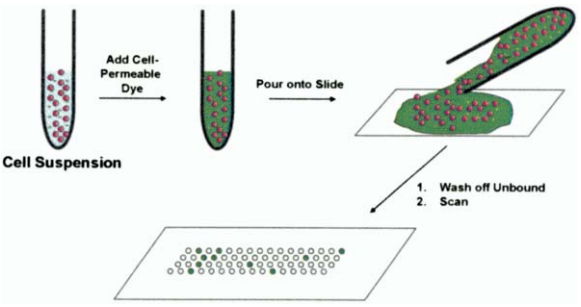

Figure 2. Schematic Representation of the Method Used to Study Carbohydrate-Cell Interactions and to Detect the Presence of Pathogens within Complex Mixtures

Either homo- or heterogeneous samples containing bacteria were stained with a cell-permeable fluorescent dye and then hybridized with the carbohydrate arrays. Fluorescent staining of the cells was necessary to increase the signal observed using a fluorescent slide reader; a weak but observable signal was found without staining the cells.

slides, ORN178 bound to mannose and not to the other carbohydrates. Furthermore, binding occurred with a signal to noise ratio of >100 despite the small size of the spots (Figure 3). CodeLink slides had the best performance since they gave the highest binding signal and the lowest background. These slides were used in all subsequent array experiments where monosaccharides were displayed. Most likely, the three-dimensional manner in which the carbohydrates were immobilized on these slides is responsible for the enhanced performance.

Other arrays that displayed mono- to nonamannosides, which were constructed as described [15], were tested for binding to ORN178 (see Supplemental Data). Results from these experiments show that ORN178 has little preference for binding to these mannosides, despite varying lengths and linkage stereochemistry. This likely reflects that recognition of mannose residues by this strain occurs through only a single mannose residue, and that stereochemistry of the linkage plays little role in binding.

The observation of cell adhesion to arrays constructed using an arraying robot with microarray-size spots is promising. A previous report studied adhesion of chicken hepatocytes and human T cells to carbohydrates arrays that were manually constructed. These spots were 1.7 mm in diameter and allowed for ~200 spots to be placed on a single slide [16]. The arrays described here show that the interactions of bacteria to carbohydrates can be studied in a high-throughput manner with the arrays. Due to the smaller spot size used here, a much larger number of interactions can be screened in parallel.

The minimal amount of carbohydrate sufficient to detect binding was determined. Analyte consumption is an important aspect for carbohydrate arrays, since materials isolated from natural sources are in short supply. Several 1 nl aliquots of serially diluted solutions of carbohydrate that ranged in concentration from 20 mM to 15 μM were arrayed. A concentration-dependent decrease in signal was observed, and delivery of as little as 20 fmol to a slide was sufficient to obtain a signal above background (Figure 4). Different concentrations of bacteria were next hybridized with the arrays to determine the bacterial detection limit. As expected, a concentration-dependent decrease in signal was observed. When 10^6 or greater ORN178 were incubated, signals were well above background (Supplemental Data); however, hybridization of 10^5 cells gave signal that approached background, thus defining the current detection limit. This sensitivity rivals or exceeds that used in methods requiring a bacterial enrichment step prior to detection [17].

Standard microscopic images were taken of ORN178 bound to three mannose-containing spots. Images show that ORN178 only adhered to these positions, they are densely covered with bacteria (Figure 4), and no bacteria are observed outside of this area. This illustrates that these slides are resistant to nonspecific adhesion of bacteria.

Assessing the Carbohydrate Binding Specificities of Different Bacterial Strains

The arrays were tested for their ability to probe differences in carbohydrate binding affinities between re-

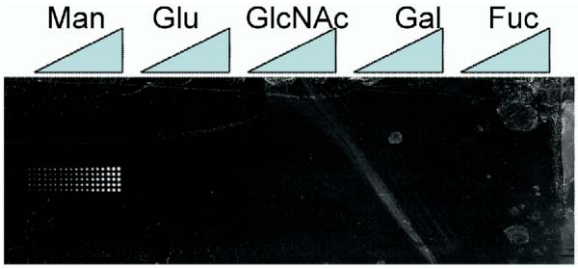

Figure 3. An Image of a Carbohydrate Array after Incubation with ORN178 that Were Stained with SYTO 83 Cell-Permeable Nucleic Acid Staining Dye

Each concentration was spotted with three rows of five spots. Each spot is the result of delivery of 1 nl of a 20 mM, 5 mM, 1.25 mM, 310 μM, 63 μM, or 15 μM carbohydrate-containing solution. The spot diameter is ~200 μm.

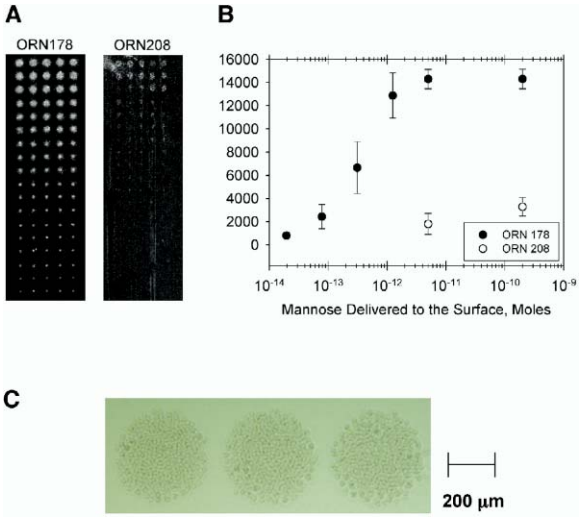

Figure 4. Adhesion of Different *E. coli* Strains to Carbohydrate Microarrays

(A) Images of mannose positions on the arrays after hybridization with mannose binding *E. coli*, ORN178, or mutant *E. coli*, ORN209, which has a greatly diminished mannose binding affinity [18].

(B) Plots of the experimental data from these two slides; the errors are the standard deviations in each measurement.

(C) A bright-field microscopic image of three spots on a carbohydrate array after hybridization with ORN178. Each spot is the result of delivering 20 pmol of mannose.

lated strains. Two *E. coli* strains were used, ORN178 and a mutant strain, ORN209, which exhibits a reduced affinity to mannose [18]. As expected, incubation of ORN209 gave a much lower signal than ORN178 (Figure 4). A 7-fold decrease was observed at the highest spot concentration, and no signal was observed at lower concentrations (Figure 4). The difference in signal is not due to differences in uptake of the dye (data not shown)

These findings demonstrate that the arrays allow for screening of mutants that have altered carbohydrate binding affinities. The ability to distinguish the different affinities of cells may have clinical applications since the virulence of many pathogens correlates with carbohydrate binding. For example, clinical isolates of *E. coli* that cause urinary tract infections bind to mannosides with a much higher affinity than strains that do not cause infections [19, 20]. Thus, the carbohydrate binding profiles determined with the array can aid in assessing pathogenicity and the design of strain-specific therapies.

Screening for Inhibitors of Carbohydrate-Cell Interactions

Antiadhesion compounds can be used as therapeutics against pathogens and other infectious agents. Our array-based method was used to measure the ability of compounds to inhibit binding of ORN178 to mannose. Inhibitors were placed in array hybridization solutions that were incubated with 10^8 ORN178 cells. Compounds tested included mannose, *p*-nitrophenyl-α-D-mannospyranoside (p-NPMan), and a water-soluble, mannose-functionalized polymer [21]. The IC_{90}s were measured and showed that mannose-functionalized polymer (50 μM) was significantly more effective at inhibiting bacterial adhesion than p-NPMan (1000 μM), which was a better inhibitor than mannose (50,000 μM) (Figure 5 and Supplemental Data).

These results agree with previous reports that showed that p-NPMan is a better adhesion inhibitor than mannose. Structural information obtained for the mannose binding pocket in *E. coli* aided the development of p-NPMan as a tight binder to *E. coli* due to forming stabilizing interactions with the aromatic residues in this protein [22]. Also, the mannose-functionalized polymer displays the carbohydrate in a multivalent manner. Multiple ligand-polymer interactions will increase the binding affinity to whole bacterial cells, since there are 100 to 400 mannose binding lectins that are displayed on the surface of *E. coli* [22, 6]. Furthermore, other multivalent scaffolds such as polymers and BSA exhibit enhanced binding to bacteria and mammalian cells compared to monovalent ligands [8, 14, 21, 23].

Carbohydrate Microarrays as a Means to Detect Bacteria

The carbohydrate array platform has the potential to be used as a biosensor because many different cell types bind to carbohydrates, and the carbohydrate binding "fingerprint" can be used to disseminate the type of bacteria present within a complex mixture [6]. Strain ORN178 was placed as a contaminant into solutions that included sheep erythrocytes and serum. SYTO 83 dye was added to these solutions, and they were directly applied to the arrays without removal of the excess dye (Figure 2). Non-cell-associated dye did not have to be removed since it did not exhibit any nonspecific binding to the array surface.

The results show that, in both cases, binding of ORN178 to the arrays is observed. Bacterial detection of ORN178 in serum showed signals well above background, which are ~2-fold lower than that observed

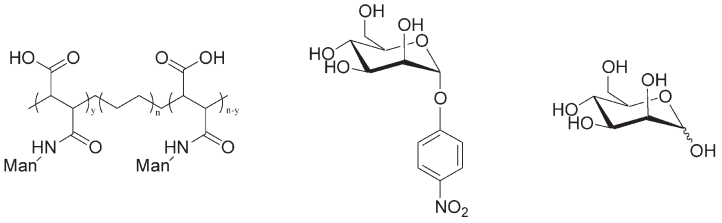

IC_{90} 50 μM 1,000 μM 50,000 μM

Figure 5. Antiadhesion Compounds Studied with the Carbohydrate Arrays

Various concentrations of inhibitors were placed into a hybridization solution that contained 10^8 ORN178, and binding to mannose-containing spots was measured. The data were then plotted versus the concentration of inhibitor (for the polymer this is moles of mannose) to determine the IC_{90}.

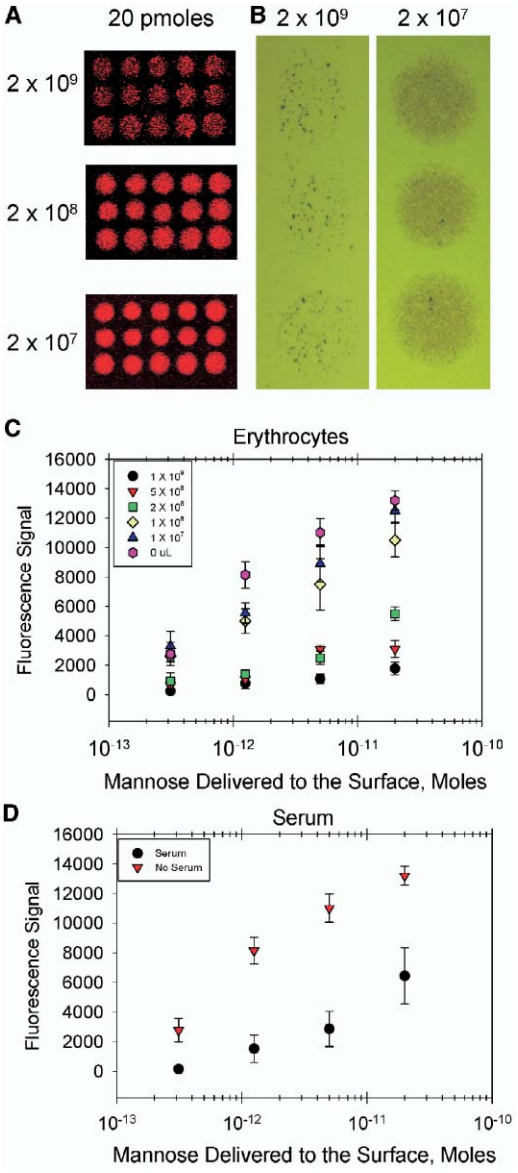

Figure 6. Image of Arrays that Have Been Hybridized with 10^8 ORN178 and Are Present in a Mixture Containing Different Concentrations of Erythrocytes

(A) A picture of the 20 nmol spots taken using a fluorescent slide scanner after hybridization of a solution containing ORN178 with various concentrations of erythrocytes. The amount of mannose that has been delivered to the surface is 20 pmoles.

(B) Bright-field microscopic image of arrays after hybridization with ORN178 and 10^9 or 10^7 erythrocytes.

(C and D) Plots for data after array hybridization of 10^8 ORN178 in a background of erythrocytes (C) and in serum (D).

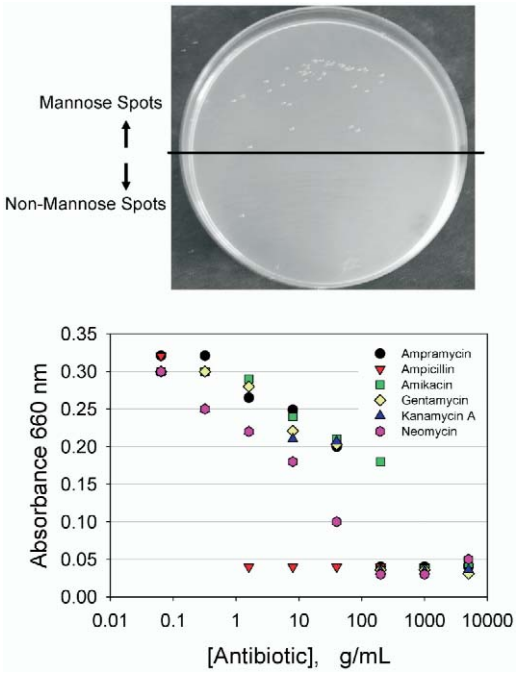

Figure 7. Growth of Bacteria that Have Been Harvested from a Carbohydrate Array and Testing for Antibacterial Susceptibility

The top shows an image of an LB plate after bacteria are harvested from an array and streaked onto the plate from mannose-containing spots and nonmannose spots. At bottom are results from antibacterial susceptibility testing of the harvested bacteria.

with a homogeneous sample (Figure 6). For experiments with erythrocytes, samples that contain equal amounts of ORN178 and erythrocytes result in signals that are equal to that observed with a homogeneous sample (Figure 6). Further addition of erythrocytes to 10-fold excess over the bacteria decreases the signal ~6-fold (Figure 6). Despite this decrease, the signal is still well above background. Brightfield microscopic images of the mannose positions on the arrays at different erythrocyte concentrations were taken to determine if decreased signal was due to less efficient uptake of the dye or erythrocyte binding to the arrays. Images clearly show that only bacteria bind and that the decrease in signal is due to decreased cell density (Figure 6).

The observation that ORN178 adhesion can be detected in complex mixtures is encouraging for the use of this array-based technique as a fast medical diagnostic. Traditional assays for pathogen detection require selective growth of bacteria in media, and such experiments may take days [17]. Recently, several platforms have been developed to accelerate this process. Colorimetric detection using bacteriophage may require a few hours [24], and other methods such as antibody staining and PCR require 6 to 48 hr to test a sample [17, 25, 26].

To further illustrate the nondestructive nature of this technique, bacteria captured on the arrays were harvested and tested for antibacterial susceptibility (Figure 7). After incubation of a homogeneous solution of ORN178 to a carbohydrate array and washing off the unbound cells, bound bacteria were removed from the array by placing an inoculating loop over the mannose-containing positions. These bacteria were streaked onto LB plates and incubated at 37°C overnight. Colonies were observed on plates after samples were harvested from mannose-containing positions. The bacteria were then further tested for antibiotic susceptibility,

including minimum inhibitory concentrations for a variety of different antibiotics (Figure 7). Thus, not only can the arrays allow for pathogen detection, but they can also be used to harvest the pathogens to allow for further testing. This is not possible with other destructive methods, such as those that require PCR.

One of the major impediments of using carbohydrate ligands to detect pathogens is the lack of specificity to different cell types. Crossreactive chemical sensors have been developed using ligands that have low specificity to circumvent this problem [27, 28]. The presence of a pathogen is determined through the binding ensemble from many different analytes. Such a scheme is used by the ~1000 different olfactory receptors that are present in the nose. The spatial nature and the ability to spot several thousand ligands on a single array using the techniques described here should simplify application of the crossreactive sensing technique.

There are several methods that have the potential to improve the detection limit of this method. These include using a different cell staining method, such as using fluorescent dyes with enhanced fluorescence properties to stain the cells or using antibodies to stain the cell membrane. Alternative array-scanning techniques have also been developed that are 100-fold more sensitive than standard slide scanners [29]. Detection down to the 100 binding events per 100 μm^2 or in the zeptomolar range can be accomplished using this instrument [29]. Studies to increase the carbohydrate arrays are under investigation and will be reported in due course.

Significance

Microarrays have proven to be a versatile technique to rapidly assess the interactions of ligands and analytes. For example, gene chips are used to determine gene expression profiles [30], chemical microarrays allow screening of combinatorial libraries [31–33], and protein arrays are used to determine protein-protein interactions [34, 35]. Carbohydrate arrays have been developed to probe carbohydrate-protein interactions [36–39, 40, 41] and to study the interactions of aminoglycoside antibiotics with their RNA targets as well as with resistance-causing enzymes [42, 43]. We demonstrate that interactions of bacteria with carbohydrates can be probed in a microarray format. These results and another report showing the binding of mammalian cells [16] to carbohydrate arrays suggest that arrays are a general platform to study the carbohydrate-cell interactions. We have also expanded the scope of these methods to include the detection of pathogens within complex mixtures. Pathogens captured by the arrays can be cultured and further tested for antibacterial susceptibility. It is likely that these assays will allow for rapid screening and testing of pathogens and aid in uncovering new roles for carbohydrates in cellular biology.

Experimental Procedures

General Methods

All aqueous solutions were made from nanopure water. Solutions used for chip hybridizations were sterile filtered through a 0.2 μm syringe filter prior to use. Each array was equipped with a hybridization chamber with dimensions of 6.5 × 2.5 cm (Grace Labs). All chemicals were purchased from Sigma Aldrich or Fluka and used without purification. Sheep erythrocytes were purchased from Sigma. Amine-coated glass slides were Coring GAPS II slides and were purchased from Corning Inc. CodeLink slides were purchased from Amersham Biosciences. NMR spectra were recorded on a 300 MHz Varian Inova spectrometer at room temperature. Mass spectra were recorded on an Agilent Series 1100 LC/MS. The running solvent for each measurement was acetonitrile/water (1/1) containing 5 mM ammonium formate. Arrays were constructed using a Perkin Elmer noncontact printer. Slides were scanned using a Scan Array 500 scanner from GSI Lumonics and quantified using Scan Array Express Software. All data are the average signal from at least 15 spots on a single array; errors are the standard deviations of those measurements. Brightfield microscopic images were taken using a Nikon Eclipse TS100 inversted microscope, with images captured using an attached digital camera.

Cell Culture

Bacterial strains ORN178 and ORN209 were a gift from Prof. P Orndorf (University of North Carolina) [18]. The ORN209 stain is a mutant derived from ORN178 where the FimH protein, which is responsible for mannose binding, is mutated to diminish mannose binding. All cultures were grown in LB media at 37°C with shaking to an OD_{660} of ~1.0 (10^8 cells/ml).

Chemical Synthesis

2′-aminoethyl-β-D-mannopyranoside, 2′-aminoethyl-β-D-glucopyranoside, 2′-aminoethyl-α–L-fucopyranoside, and 2′-aminoethyl-β-D-galactopyranoside were synthesized according to published procedures [44, 45].

***2′*-Azidoethyl, 3,4,5-Tri-O-Acetyl-2-Acetylamino-2-Deoxy-α-D-Glucopyranoside**

To a solution of *N*-acetyl-D-glucosamine (3.2 g, 14 mmol) was added 2-chloroethanol (20 ml, 300 mmol) and Dowex resin 50 × 8 (2.0 g), and the solution was heated to 80°C for 2 hr. The reaction was filtered to remove the resin, and the excess 2-cloroethanol was removed by distillation on a rotary evaporator. The crude mixture was added to pyridine (20 ml), acetic anhydride (10 ml), and a catalytic amount of 4-dimethylaminopyridine, and the reaction was stirred for 2 hr. Approximately 100 ml of a mixture of water and ice (~1:1) was added to the reaction mixture, and the aqueous solution was extracted with 3 × 100 ml dichloromethane. The organic layer was subsequently washed with 1 N HCl, brine, and dried over Na_2SO_4. The product was purified by silica gel flash column chromatography using EtOAc:hexanes (5:3).

To a solution of 2′-chloroethanol, 3,4,5-tri-*O*-acetyl-2-acetylamino-2-deoxy-α–D-glucopyranoside (1.7 g, 4 mmol) was added sodium azide (2.7 g, 40 mmol) and sodium iodide (0.6 g, 0.4 mmol) in 18 ml DMF, and the reaction was heated at 80°C overnight. The DMF was evaporated and the crude mixture was resuspended in 200 ml CH_2Cl_2, washed with H_2O (150 ml), brine (3 × 150 ml), dried with Na_2SO_4, and concentrated. The product was purified by silica gel flash column chromatography using EtOAc:hexanes (7:5) to afford 1.50 g of 2′-azidoethyl-3,4,5-tri-*O*-acetyl-2-acetylamino-2-deoxy-α-D-glucopyranoside (27% over three steps). ^1H NMR (300 MHz, $CDCl_3$): δ 5.81 (d, *J* = 9.3 Hz, 1H), 5.19 (t, *J* = 8.1 Hz, 1H), 5.07 (d, *J* = 9.6 Hz, 1H), 4.85 (d, *J* = 3.3 Hz, 1H), 4.32 (td, *J* = 10.5, 3.3 Hz, 1H), 4.19 (m, 1H), 4.04 (m, 1H), 3.93–3.83 (m, 2H), 3.61 (m, 1H), 3.51 (m, 1H), 3.35 (m, 1H), 2.04 (s, 3H), 1.98 (s, 3H), 1.96 (s, 3H), 1.89 (s, 3H). ^{13}C (75 MHz, $CDCl_3$): δ 171.4, 170.8, 170.3, 169.5, 97.7, 71.1, 68.2, 67.6, 62.1, 51.8, 50.5, 23.2, 20.8. ESI-MS (positive mode) = 417.3 ($M + H^+$).

***2′*-Aminoethanyl-2-Acetylamino-2-Deoxy-α-D-Glucopyranoside**

To 2′-azidoethyl-3,4,5-tri-*O*-acetyl-2-acetylamino-2-deoxy-α-D-glucopyranoside (1.5 g, 4 mmol) in 20 ml methanol was added a catalytic amount of sodium methoxide (0.05 g, 0.25 eq). The reaction was stirred for 2 hr and neutralized with Dowex 50× resin. The solution was filtered and concentrated.

2′-Azidoethyl-2-acetylamino-2-deoxy-α-D-glucopyranoside was dissolved in 30 ml methanol and stirred overnight under an atmosphere of hydrogen in the presence of 100 mg of Pd/C. The reac-

tion mixture was filtered through a pad of celite and concentrated. The compound was isolated without purification to yield 1.2 g of product. ^{1}H NMR (300 MHz, H_2O): δ 4.85 (d, J = 3.3 Hz, 1H), 4.80–3.65 (m, 6H), 3.45 (m, 2H), 2.80 (m, 2H), 2.01 (s, 3H); ^{13}C (75 MHz, H_2O): δ 174.44, 97.09, 71.89, 71.03, 70.27, 69.37, 60.57, 53.70, 40.08, 21.82. ESI-MS (positive mode) = 265.0 ($M + H^+$).

Carbohydrate Arrays

Carbohydrate microarrays were constructed using a robotic noncontact printer. For arraying onto CodeLink slides, sugars were dissolved in 50 mM sodium phosphate buffer (pH 9.0). For the other slides, carbohydrates were dissolved in a 25% aqueous solution of DMF as described previously [42, 43]. After printing, slides were immediately placed in a sealed chamber that contained a slurry of sodium chloride in water to result in an atmosphere of ~70% humidity. After incubation overnight in the chamber, slides were washed several times with distilled water to remove the unreacted carbohydrates from the surface. Remaining amine groups were quenched by placing slides in a solution preheated to 50°C that contained 100 mM ethanolamine in 50 mM sodium phosphate buffer (pH 9.0) for at least 30 min. Slides were removed from this solution, washed exhaustively with deionized water, briefly shaken in ethanol, dried by centrifugation, and stored in a dry box until use.

Cell Staining and Array Hybridization

Aliquots of the bacterial cultures were centrifuged to isolate the cells and were washed twice with an equal volume of PBS buffer (pH 7.2). After each wash, bacteria were resuspended and centrifuged. Cells were fluorescently stained with SYTO 83 orange-fluorescent cell-permeable nucleic acid dye (Molecular Probes, Eugene, OR). Dye was added to a 1 ml suspension of bacteria at a concentration of 50 μM in PBS buffer and shaken for 1 hr. After incubation, the cell suspension was centrifuged, isolated, and washed twice with 1 ml PBS buffer. Solutions of bacteria that contained either serum or erythrocytes were suspended in PBS buffer, stained with 50 μM of SYTO 83 dye, and incubated for 30 min. After staining, samples were directly applied to the arrays. Dye that was not cell associated did not nonspecifically bind to the CodeLink slides.

Each array was equipped with a hybridization chamber, and then 800 µl solution of *E. coli* in PBS buffer that contained 1 mM $CaCl_2$ and 1 mM $MnCl_2$ was applied to the surface. The arrays were gently shaken on a platform for 1 hr at room temperature. After incubation, the hybridization chamber was removed, and unbound cells were washed away from the array by dipping it into a 50 ml solution of the hybridization buffer. This step was repeated twice, and the buffer was changed between washings. A final wash with nanopure water was used to remove salts from the array. Slides were then briefly centrifuged at ~1000 rpm for 1 min to dry the arrays. The arrays were then scanned using a fluorescent slide reader.

Harvesting Bacteria from an Array and Antibiotic Testing

Strain ORN178 was stained with a 50 μM solution of SYTO 62 dye as described above and incubated with the array, unbound bacteria was washed off, and the slides were scanned. Positions on the array where the various carbohydrates were immobilized were mapped out using the fluorescent scan of the array. An inoculating loop was scraped over each position where a carbohydrate had been delivered to harvest bound *E. coli*. The loop was then streaked onto LB plates and incubated at 37°C overnight. After incubation, many (hundreds to thousand) colonies were observed when the samples were taken from the mannose-containing positions, and few (two) to no colonies were observed from samples taken at other positions. Bacteria from the LB plate were then transferred to LB broth and grown. The number of bacteria were diluted to OD_{660} of 0.001 and placed into a 96-well plate with or without serially diluted concentrations of antibiotics. Plates were then grown for 24 hr at 37°C, the culture was pippeted up and down to resuspend the cells in the media, and OD_{660} were immediately taken using a Sepctra Max 250 microplate reader. Dose-response curves were then plotted as the absorbance at 660 nm versus the concentration of antibiotic.

Supplemental Data

Data for studies of antiadhesion inhibitors, for testing a series of high-mannosides for binding to *E. coli* ORN178, and for measuring the detection limit for *E. coli* binding to mannose on the arrays are included in the Supplemental Data available at http://www.chembiol.com/cgi/content/full/11/12/1701/DC1/.

Acknowledgments

The authors thank Dr. Dan Ratner for the gift of the high mannose array and Prof. Orndorff for the gift of the *E. coli* strains. A Roche Research Foundation Postdoctoral Fellowship (to M.D.D), GlaxoSmithKline (Scholar Award to P.H.S.), the Alfred P. Sloan Foundation (Fellowship to P.H.S.), Merck (Academic Development Award to P.H.S.), and ETH are acknowledged for financial support. We also thank the Functional Genomics Center, Zürich and Dr. Jens Sobek for construction of microarrays.

Received: July 6, 2004
Revised: September 22, 2004
Accepted: October 7, 2004
Published: December 17, 2004

References

1. Kleene, R., and Schachner, M. (2004). Glycans and neural cell interactions. Nat. Rev. Neurosci. *5*, 195–208.
2. Hakomori, S., and Handa, K. (2002). Glycosphingolipid-dependent cross-talk between glycosynapses interfacing tumor cells with their host cells: essential basis to define tumor malignancy. FEBS Lett. *531*, 88–92.
3. Smith, A.E., and Helenius, A. (2004). How viruses enter animal cells. Science *304*, 237–242.
4. Karlsson, K.A. (1999). Bacterium-host protein-carbohydrate interactions and pathogenicity. Biochem. Soc. Trans. *27*, 471–474.
5. Kiessling, L.L., Gestwicki, J.E., and Strong, L.E. (2000). Synthetic multivalent ligands in the exploration of cell-surface interactions. Curr. Opin. Chem. Biol. *4*, 696–703.
6. Mammen, M., Choi, S.K., and Whitesides, G.M. (1998). Polyvalent interactions in biological systems: Implications for design and use of multivalent ligands and inhibitors. Angew. Chem. Int. Ed. Engl. *37*, 2755–2794.
7. Autar, R., Khan, A.S., Schad, M., Hacker, J., Liskamp, R.M., and Pieters, R.J. (2003). Adhesion inhibition of F1C-fimbriated *Escherichia coli* and *Pseudomonas aeruginosa* PAK and PAO by multivalent carbohydrate ligands. ChemBioChem *4*, 1317–1325.
8. Nagahori, N., Lee, R.T., Nishimura, S., Page, D., Roy, R., and Lee, Y.C. (2002). Inhibition of adhesion of type 1 fimbriated Escherichia coli to highly mannosylated ligands. ChemBioChem *3*, 836–844.
9. Reuter, J.D., Myc, A., Hayes, M.M., Gan, Z., Roy, R., Qin, D., Yin, R., Piehler, L.T., Esfand, R., Tomalia, D.A., et al. (1999). Inhibition of viral adhesion and infection by sialic-acid-conjugated dendritic polymers. Bioconjug. Chem. *10*, 271–278.
10. Choi, S.K., Mammen, M., and Whitesides, G.M. (1997). Generation and in situ evaluation of libraries of poly(acrylic acid) presenting sialosides as side chains as polyvalent inhibitors of influenza-mediated hemagglutination. J. Am. Chem. Soc. *119*, 4103–4111.
11. Sigal, G.B., Mammen, M., Dahmann, G., and Whitesides, G.M. (1996). Polyacrylamides bearing pendant alpha-sialoside groups strongly inhibit agglutination of erythrocytes by influenza virus: The strong inhibition reflects enhanced binding through cooperative polyvalent interactions. J. Am. Chem. Soc. *118*, 3789–3800.
12. Charych, D.H., Nagy, J.O., Spevak, W., and Bednarski, M.D. (1993). Direct colorimetric detection of a receptor-ligand interaction by a polymerized bilayer assembly. Science *261*, 585–588.
13. Ma, Z.F., Li, J.R., Liu, M.H., Cao, J., Zou, Z.Y., Tu, J., and Jiang,

L. (1998). Colorimetric detection of Escherichia coli by polydiacetylene vesicles functionalized with glycolipid. J. Am. Chem. Soc. *120*, 12678–12679.

14. Disney, M.D., Zheng, J., Swager, T.M., and Seeberger, P.H. (2004). Detection of bacteria with carbohydrate-functionalized fluorescent polymers. J. Am. Chem. Soc. *126*, 13343–13346.
15. Adams, E.W., Ratner, D.M., Bokesch, H.R., McMahon, J.B., O'Keefe, B.R., and Seeberger, P.H. (2004). Oligosaccharide and glycoprotein microarrays as tools in HIV glycobiology; glycan-dependent gp120/protein interactions. Chem. Biol. *11*, 875–881.
16. Nimrichter, L., Gargir, A., Gortler, M., Altstock, R.T., Shtevi, A., Weisshaus, O., Fire, E., Dotan, N., and Schnaar, R.L. (2004). Intact cell adhesion to glycan microarrays. Glycobiology *14*, 197–203.
17. Willis, R.C. (2004). Improved molecular techniques help researchers diagnose microbial conditions. Mod. Drug Discov. *7*, 36–42.
18. Harris, S.L., Spears, P.A., Havell, E.A., Hamrick, T.S., Horton, J.R., and Orndorff, P.E. (2001). Characterization of *Escherichia coli* type 1 pilus mutants with altered binding specificities. J. Bacteriol. *183*, 4099–4102.
19. Sokurenko, E.V., Chesnokova, V., Dykhuizen, D.E., Ofek, I., Wu, X.R., Krogfelt, K.A., Struve, C., Schembri, M.A., and Hasty, D.L. (1998). Pathogenic adaptation of Escherichia coli by natural variation of the FimH adhesin. Proc. Natl. Acad. Sci. USA *95*, 8922–8926.
20. Sokurenko, E.V., Chesnokova, V., Doyle, R.J., and Hasty, D.L. (1997). Diversity of the Escherichia coli type 1 fimbrial lectin. Differential binding to mannosides and uroepithelial cells. J. Biol. Chem. *272*, 17880–17886.
21. Gestwicki, J.E., Cairo, C.W., Strong, L.E., Oetjen, K.A., and Kiessling, L.L. (2002). Influencing receptor-ligand binding mechanisms with multivalent ligand architecture. J. Am. Chem. Soc. *124*, 14922–14933.
22. Sharon, N. (1987). Bacterial lectins, cell-cell recognition and infectious disease. FEBS Lett. *217*, 145–157.
23. Gestwicki, J.E., Strong, L.E., Cairo, C.W., Boehm, F.J., and Kiessling, L.L. (2002). Cell aggregation by scaffolded receptor clusters. Chem. Biol. *9*, 163–169.
24. Park, D.J., Drobniewski, F.A., Meyer, A., and Wilson, S.M. (2003). Use of a phage-based assay for phenotypic detection of mycobacteria directly from sputum. J. Clin. Microbiol. *41*, 680–688.
25. Waites, K.B., Smith, K.R., Crum, M.A., Hockett, R.D., Wells, A.H., and Hook, E.W., III. (1999). Detection of Chlamydia trachomatis endocervical infections by ligase chain reaction versus ACCESS Chlamydia antigen assay. J. Clin. Microbiol. *37*, 3072–3073.
26. Andreotti, P.E., Ludwig, G.V., Peruski, A.H., Tuite, J.J., Morse, S.S., and Peruski, L.F., Jr. (2003). Immunoassay of infectious agents. Biotechniques *35*, 850–885.
27. Cho, E.J., and Bright, F.V. (2002). Pin-printed chemical sensor arrays for simultaneous multianalyte quantification. Anal. Chem. *74*, 1462–1466.
28. Michael, K.L., Taylor, L.C., Schultz, S.L., and Walt, D.R. (1998). Randomly ordered addressable high-density optical sensor arrays. Anal. Chem. *70*, 1242–1248.
29. Pawlak, M., Schick, E., Bopp, M.A., Schneider, M.J., Oroszlan, P., and Ehrat, M. (2002). Zeptosens' protein microarrays: a novel high performance microarray platform for low abundance protein analysis. Proteomics *2*, 383–393.
30. Brown, P.O., and Botstein, D. (1999). Exploring the new world of the genome with DNA microarrays. Nat. Genet. *21*, 33–37.
31. Hergenrother, P.J., Depew, K.M., and Schreiber, S.L. (2000). Small-molecule microarrays: Covalent attachment and screening of alcohol-containing small molecules on glass slides. J. Am. Chem. Soc. *122*, 7849–7850.
32. Kuruvilla, F.G., Shamji, A.F., Sternson, S.M., Hergenrother, P.J., and Schreiber, S.L. (2002). Dissecting glucose signalling with diversity-oriented synthesis and small-molecule microarrays. Nature *416*, 653–657.
33. MacBeath, G., Koehler, A.N., and Schreiber, S.L. (1999). Printing small molecules as microarrays and detecting protein-ligand interactions en masse. J. Am. Chem. Soc. *121*, 7967–7968.
34. MacBeath, G., and Schreiber, S.L. (2001). Proteomics comes to the surface. Nat. Biotechnol. *19*, 828–829.
35. MacBeath, G., and Schreiber, S.L. (2000). Printing proteins as microarrays for high-throughput function determination. Science *289*, 1760–1763.
36. Fazio, F., Bryan, M.C., Blixt, O., Paulson, J.C., and Wong, C.H. (2002). Synthesis of sugar arrays in microtiter plate. J. Am. Chem. Soc. *124*, 14397–14402.
37. Fukui, S., Feizi, T., Galustian, C., Lawson, A.M., and Chai, W. (2002). Oligosaccharide microarrays for high-throughput detection and specificity assignments of carbohydrate-protein interactions. Nat. Biotechnol. *20*, 1011–1017.
38. Park, S., and Shin, I. (2002). Fabrication of carbohydrate chips for studying protein-carbohydrate interactions. Angew. Chem. Int. Ed. Engl. *41*, 3180–3182.
39. Houseman, B.T., and Mrksich, M. (2002). Carbohydrate arrays for the evaluation of protein binding and enzymatic modification. Chem. Biol. *9*, 443–454.
40. Ratner, D.M., Adams, E.W., Su, J., O'Keefe, B.R., Mrksich, M., and Seeberger, P.H. (2004). Probing protein-carbohydrate interactions with microarrays of synthetic oligosaccharides. ChemBioChem *5*, 379–382.
41. Bryan, M.C., Plettenburg, O., Sears, P., Rabuka, D., Wacowich-Sgarbi, S., and Wong, C.H. (2002). Saccharide display on microtiter plates. Chem. Biol. *9*, 713–720.
42. Disney, M.D., and Seeberger, P.H. (2004). Aminoglycoside microarrays to explore interactions of antibiotics to RNAs and proteins. Chemistry (Easton) *10*, 3308–3314.
43. Disney, M.D., Magnet, S., Blanchard, J.S., and Seeberger, P.H. (2004). Aminoglycoside microarrays to study antibiotic resistance. Angew. Chem. Int. Ed. Engl. *43*, 1591–1594.
44. Ni, J., Singh, S., and Wang, L.X. (2003). Synthesis of maleimide-activated carbohydrates as chemoselective tags for site-specific glycosylation of peptides and proteins. Bioconjug. Chem. *14*, 232–238.
45. Chernyak, A.Y., Sharma, G.V.M., Kononov, L.O., Krishna, P.R., Levinsky, A.B., Kochetkov, N.K., and Rao, A.V.R. (1992). 2-Azidoethyl glycosides: glycosides potentially useful for the preparation of neoglycoconjugates. Carbohydr. Res. *223*, 303–309.